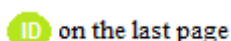




Molecular structure, frontier molecular orbitals, NBO, MESP and thermodynamic properties of 5,12-dibromo perylene with DFT calculation methods

Murat AKMAN¹, Ahmet Cagri ATA^{1,*}, Ümit YILDİKO², İsmail CAKMAK¹



¹Faculty of Arts and Sciences, Department of Chemistry, Kafkas University, Kars, 36100, Turkey

²Architecture and Engineering Faculty, Department of Bioengineering, Kafkas University, Kars, 36100, Turkey

Received: 27 February 2020; Final revised: 03 May 2020; Accepted: 05 May 2020

*Corresponding author e-mail: ahmetata1024@gmail.com

Citation: Akman, M.; Ata, A. C.; Yildiko, Ü.; Cakmak, İ. *Int. J. Chem. Technol.* 2020, 4 (1), 49-59.

ABSTRACT

Perylene-3,4,9,10-tetracarboxylic dianhydride (PTCDA) has been used as industrial pigments for many years. This perspective makes it important to determine the synthesis and physical properties of PTCDA derivatives and their functional properties for application as electron acceptors in organic transistors. In the gas phase, the quantum chemical study of the 5,12-dibromoperylene compound was performed using the basic set of LanL2DZ and 6-311G of the density function theory (DFT)-B3LYP method. Because basic set of LanL2DZ and 6-311G of the density function theory (DFT)-B3LYP method are predicted to yield more efficient and verifiable results than others. ¹H-NMR, ¹³C-NMR, HOMO-LUMO analysis, dipole moment, molecular electrostatic surface potential (MESP) and natural orbital bond (NBO) analysis of the molecule were carried out. The results were shown with graphs, tables and figures. In the comparison of ¹H-NMR, ¹³C-NMR results with the experimental values, B3LYP 6-311G gave more successful results. The nonlinear optical properties of the compound were determined.

Keywords: PTCDA derivatives, DBP, DFT, LanL2DZ.

5,12-dibromo perilenin DFT hesaplama yöntemleri ile moleküler yapısı, sınır moleküler orbitalleri, NBO, MESP ve termodinamik özellikleri

ÖZ

Perylene-3,4,9,10-tetrakarboksilik dianhidrit (PTCDA) birçok yıldan beri endüstriyel pigmentler olarak kullanılmaktadır. Bu bakış açısı, PTCDA türevlerinin sentez ve fiziksel özelliklerinin ve bunların organik transistörlerde elektron alıcısı olarak uygulanacak fonksiyonel özelliklerinin belirlenmesini önemli kılmaktadır. Gaz fazında, 5,12-Dibromoperilylen bileşiğinin kuantum kimyasal incelemesi, yoğunluk fonksiyonu teorisi (DFT) -B3LYP yönteminin temel LanL2DZ ve 6-311G seti kullanılarak gerçekleştirildi. Çünkü, yoğunluk fonksiyon teorisinin temel LanL2DZ ve 6-311G (DFT)-B3LYP yönteminin diğerlerinden daha verimli ve doğrulanabilir sonuçlar vereceği tahmin edilmektedir. ¹H-NMR, ¹³C-NMR, HOMO-LUMO analizi, dipol momenti, moleküler elektrostatik yüzey potansiyeli (MESP) ve molekülün doğal orbital bağı (NBO) analizi yapıldı. Sonuçlar grafikler, tablolar ve şekillerle gösterildi. ¹H-NMR, ¹³C-NMR sonuçlarının deneysel değerlerle karşılaştırılmasında B3LYP 6-311G daha başarılı sonuçlar verdi. Bileşiğin doğrusal olmayan optik özellikleri belirlendi.

Anahtar Kelimeler: PTCDA türevleri, DBP, DFT, LanL2DZ.

1. INTRODUCTION

Organic semiconductors and aromatic compounds are used in the production of many electronic devices.¹ thermal,²⁻³ electrical, optical,⁴⁻⁵ and properties of these materials can be improved by using new functional

organic groups. Thus, it will provide the opportunity to design low-cost material for device applications.⁶ The subject of our study may be perilen-3,4,9,10-tetracarboxylic dianhydride (PTCDA), organic type semiconductor based batteries and candidate materials for organic batteries.⁷⁻⁸ Battery systems, one of the most

important needs of today's electronic technology, are important in providing effective results.

However, in addition to its use as an important industrial pigment, PTCDAs exhibit many interesting properties such as near-unit products that enable them to be used in many new advanced applications, high photochemical stability and high electron uptake.⁹⁻¹⁰ To date, PTCDAs have been utilized in a variety of electronic and optical applications, such as fluorescent solar collectors, electro-photographic devices, dye lasers, organic photovoltaic cells,¹⁰ and optical energy limiters, due to their special physical, optical and electronic properties, in addition to being associated with their derivatives. In many of these applications, it plays a key role in the relatively pure and reversible reduction of PTCDAs. These pure reductions have led to their widespread use in basic research on photo-induced energy and electron transfer processes, the combination of easily identifiable excited state, anion and dianion absorption spectra. PTCDA derivatives,¹⁰ an important monomer in the preparation of polymer materials, are indispensable. Density functional theory (DFT) is one of the most popular and versatile methods available in quantum chemistry and is used in many studies.¹¹⁻¹⁶

In this study, the ab-initio calculations of the 5,12-dibromoperylene (DBP) molecule, which was synthesized by our group, were made in Gaussian 09 program. For DBP molecule, it was first plotted in ChemBioDraw program and minimized by SYBL2 (mol2) method with Chem3D program. DBP was optimized by using DFT/LanL2DZ and 6-311G basis set. The ¹H NMR and ¹³C NMR spectra of the molecule were compared with the experimental results.

2. MATERIALS AND METHODS

3.1. Computer calculations

The DBP molecule synthesized by our group was first drawn in ChemBioDraw for each molecule for ab-initio calculations in Gaussian 09 program¹⁷ and minimized by SYBL2 (mol2) method with Chem3D program. Minimized molecules were given to Gaussian 09 program and ab-initio calculations were made for each structure.

3. RESULTS AND DISCUSSION

3.1. Geometry optimization

In both research and industrial settings, the primary starting material for synthesizing PCTDA was optimized using powerful computational software of Gaussian 09 and by DFT / B3LYP and DBP methods

with 6-311 ++ G (d, 2p) and LanL2DZ basis sets. Then the value of bond lengths amounts and angles between its constituent atoms were compared with each other from optimized structure and using two mentioned methods.¹⁸ Calculations were made using the Density Function Theory / Becke-3- LeeYang-Parr (DFT / B3LYP)^{19,20} method, which is a quantum mechanical method. The main idea that DFT is based on is to determine the energy of the molecule by using electron density instead of the wave function. The superiority of DFT methods is that the electron correlations are included in the calculations and the results obtained are in better agreement with the experimental results. It also requires less calculation. DFT is a variational method. The most used method in the DFT method is BLYP (Becke, Lee, Yang and Parr) and the B3LYP method formed by the modification of BLYP. Therefore, LanL2DZ (Hay and Wadt's effective core potential) basic set of DFT / B3LYP method was used in our calculations. In very large nuclei, near-nucleus electrons are treated as approximately effective nucleus potential (ECPs).²¹ This behavior includes some relative effects that are important for these atoms. Since the LanL2DZ basic set is the best known, this set was used in our calculations. DBP optimized baseline structure and total energy conversion are given in Figure 1. Optimized bond length parameters of the molecule calculated with the basis set of 6-311G (d, p) and LanL2DZ of DFT-B3LYP are listed in Table 1. Comparison of two optimized methods of DBP compound was performed. With this optimization, it gives the molecule the minimum energy. A method is presented for generating a good initial guess of a transition path between given initial and final states of a system without evaluation of the energy. The bond lengths and bond angles in the aromatic phenyl rings are of normal value.

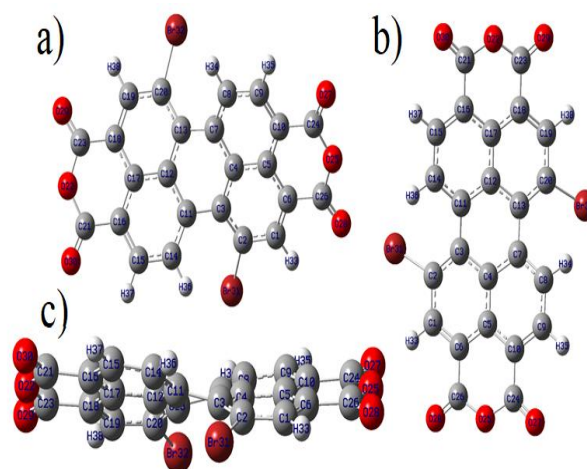


Figure 1. Optimized structures of the DBP compound from a different perspective.

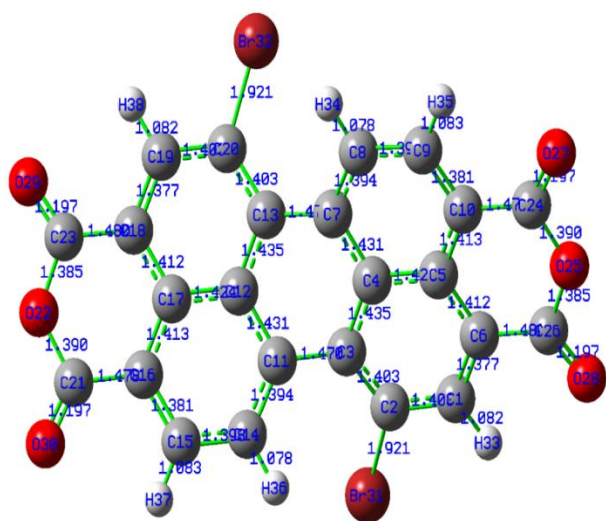


Figure 2. Optimized bond lengths of the DBP compound

C-C bond lengths is 1.37-1.48 Å for DFT and 1.39 to 1.48 Å for LanL2DZ, and 1.19 to 1.38 Å for these values for C-O belong to the oxygen atom between the two phenyl rings. The C-H lengths in the aromatic ring are 1.07-1.08 Å and the C-Br length is 1.93 Å. All C-C-C angles range from 118° to 126°. The C-C-H angle in the compound is 119°-121°, C-C-O 117°-124°, Br-C-C 114°-124° and O-C-O 119°. In our study, the theoretically calculated molecule shows that the bond lengths and bond angles are compatible with the literature data and the results are consistent.^{22,23} Some of the dihedral angles show negative results in the degree of angle in the Gaussian 09 program when atoms are selected as dihedral bonds. These calculated numbers depend on the state of the atoms in the bonds and in their place were valuable. There are very small differences between the DFT and LanL2DZ values.

Table 1. Theoretically obtained BL (Å^o) and BA (°) of the molecule

BL(Å ^o)	6-311G	LanL2DZ	BA (°)	6-311G	LanL2DZ
C2-C1	1.40276	1.41287	C3-C2-C1	121.87902	121.79513
C6-C1	1.37715	1.39016	C1-C2-Br31	113.47705	113.18623
C1-H33	1.08169	1.08493	C1-C6-C5	119.96614	119.95634
C2-C3	1.40269	1.41388	C1-C6-C26	119.49842	119.00333
C2-Br31	1.92060	1.97217	C2-C1-C6	120.46872	120.50160
C4-C5	1.42377	1.43324	C2-C1-H33	120.33833	120.63480
C4-C7	1.43137	1.44185	C3-C2-C1	121.87902	121.79513
C8-H34	1.07783	1.07995	C3-C2-Br31	124.54819	124.86472
C9-C10	1.38099	1.39355	C6-C26-O25	116.71404	116.39006
C14-H36	1.07783	1.07997	C6-C26-O28	124.90317	125.31475
C15-C16	1.38098	1.39357	C10-C9-H35	119.34112	119.20788
C15-H37	1.08274	1.08543	C10-C24-O25	116.90499	116.55425
O22-C23	1.38496	1.41655	O22-C21-O30	118.04399	117.94383
C23-O29	1.19732	1.23084	O22-C23-O29	118.38186	118.29606
C24-O25	1.38960	1.42158	C24-O25-C26	125.53681	125.11154
O25-C26	1.38494	1.41657	O25-C24-O27	118.04343	117.94444
C26-O28	1.19732	1.23084	O25-C26-O28	118.38271	118.29512

Theoretically calculated values of some perylene compounds can give an idea about the geometry of molecular changes.²⁴

Table 1 shows optimized bond lengths and bond angles based on DFT-B3LPY / 6-311G (d, p) and LanL2DZ. The difference is very small and shows a good fit between the two systems. Table 2 shows theoretically obtained dihedral bond angles of the molecule.

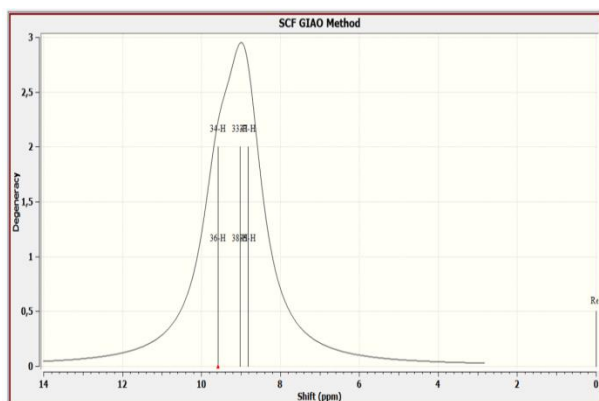
3.2. ¹³C NMR ve ¹H NMR spectral analysis

NMR spectroscopy is used to determine the content and purity of a sample. Also, molecular structure, conformation, solubility etc. parameters can be used to estimate. ¹³C NMR and ¹H NMR chemical shifts were calculated by DFT-B3LPY / 6-311G (d, p) and LanL2DZ methods in the gas phase of the conformers of DBP.²⁵

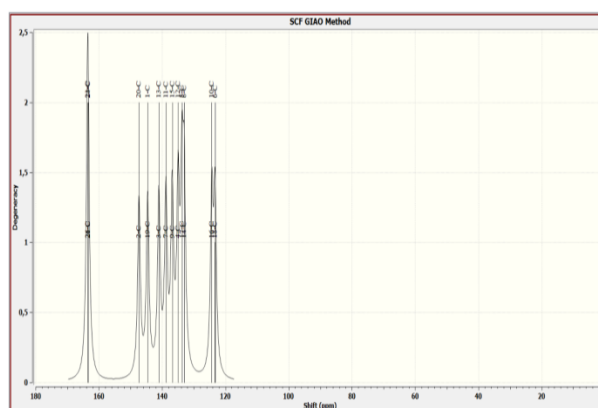
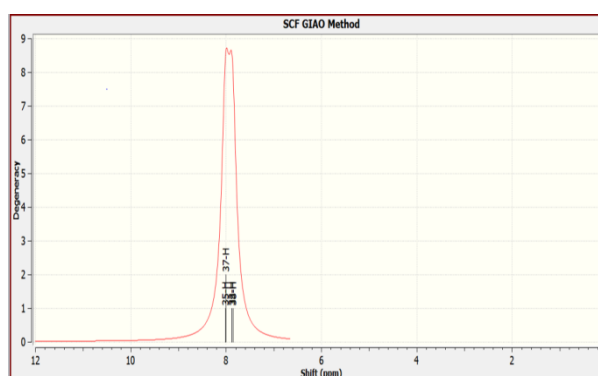
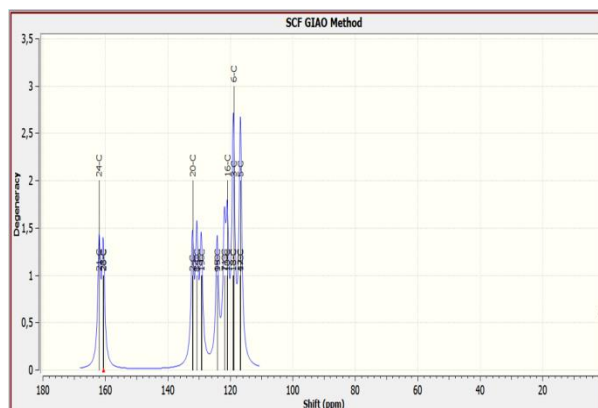
Table 2. Theoretically obtained dihedral bond angles of the molecule ($^{\circ}$).

Dihedral Angles	6-311G	LanL2DZ
C1-C2-C3-C4	9.29497	9.27679
C1-C2-C3-C11	-168.94056	-168.52963
C1-C6-C5-C4	1.20436	1.70608
C1-C6-C26-O25	-179.70499	179.39721
C1-C6-C26-O28	0.18758	-0.69970
C1-C6-C5-C10	-178.94833	-178.48016
C3-C2-C1-H33	178.57447	178.37931
C3-C4-C5-C10	-171.73565	-172.50192
C3-C4-C7-C8	169.25017	169.88180
C3-C4-C7-C13	-8.90052	-8.51608
C3-C11-C14-H36	3.77654	4.32008
C4-C3-C2-Br31	-166.91181	-165.90146
C5-C6-C1-H33	175.96350	175.90540
C5-C6-C26-O25	2.11829	1.29264
C5-C6-C26-O28	-177.98914	-178.80428
C5-C10-C24-O25	2.22711	1.35794
C4-C3-C2-Br31	-166.91181	-165.90146
C6-C1-C2-Br31	176.34344	175.16669
H33-C1-C2-Br31	-4.83131	-5.92354
H38-C19-C20-Br32	-4.83676	-5.89966
H34-C8-C9-H35	0.21872	-0.42258
H37-C15-C14-H36	0.21484	-0.42420

In this study, NMR chemical shifts were calculated using GIAO-B3LYP method and 6-311G + (d, p) basis set. The theoretical spectra obtained from the calculation results are shown in Figures 3-6.

**Figure 3.** DBP DFT ^1H NMR spectra.

Experimentally obtained ^1H NMR and ^{13}C NMR spectra are presented in Figures 7 and 8. The experimental and theoretical ^1H NMR and ^{13}C NMR chemical shifts (ppm) in Tables 3 and 4 are listed and compared. ^{13}C NMR chemical shift graph of the comparison results is given in Figure 9. The DBP molecule has 6 H in the phenyl ring.

**Figure 4.** DBP DFT ^{13}C NMR spectra.**Figure 5.** DBP LanL2DZ ^1H NMR spectra.**Figure 6.** DBP LanL2DZ ^{13}C NMR spectra.

The chemical shift of these hydrogens was observed in the range of 8.89-9.56 ppm. Calculation for 6-311 G was found (H37-H35), (H33-H38) and (H34-H36) 8.92-8.10, 9.03-7.84 and 9.56-13.3 ppm. Since the calculation is in the gas phase, there may be deviations from the actual value. The chemical shift (ppm) of the hydrogens bonded to C-H groups was 8.91-8.00 ppm.

The electronic environment of the proton can have a major impact on the chemical shift.²⁶ NMR results are consistent with the results obtained in previous studies. The regression graph shown in Figure 10 was found to be a good match for ¹³C-NMR. Correlation was calculated as R = 0.97 (6-311G) and R = 0.92 (LanL2DZ).

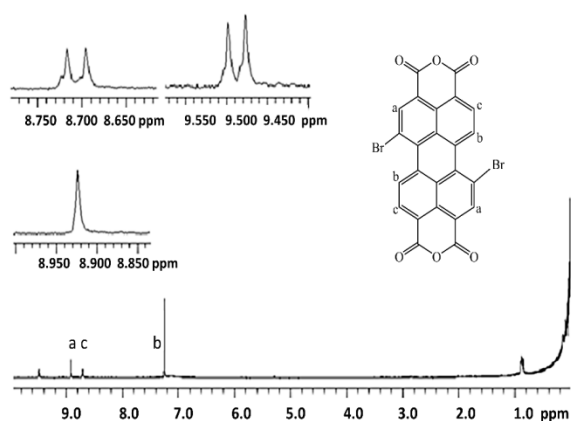


Figure 7. DBP experimental ¹H NMR spectra.

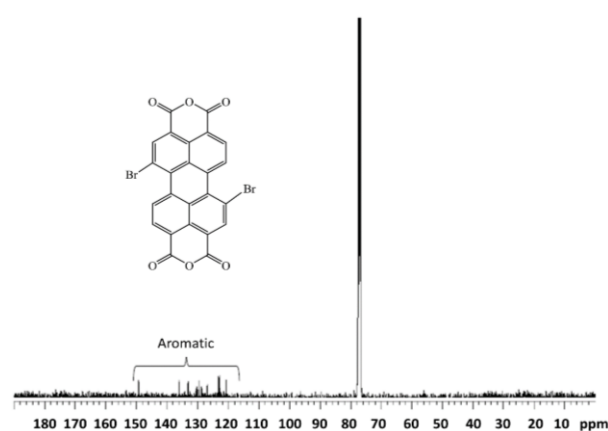


Figure 8. DBP ¹³C NMR spectra.

3.3. Frontier molecular orbitals

The basic electronic parameters of the molecule can be calculated by predicting the highest occupied molecular orbital (HOMO) and the lowest unoccupied molecular orbital (LUMO) and bandgap. HOMO which can function as an electron donor, and LUMO which have enough space to accept electrons and can act as an electron acceptor are border orbitals.²⁷⁻²⁹ Figures 11 and 12 show the densities of the orbital representation of HOMO and LUMO for the DBP molecule. LUMO₊₁ and HOMO₋₁ graphs of the compound were also obtained. HOMO -6.97 eV - LUMO -4.42 eV for the

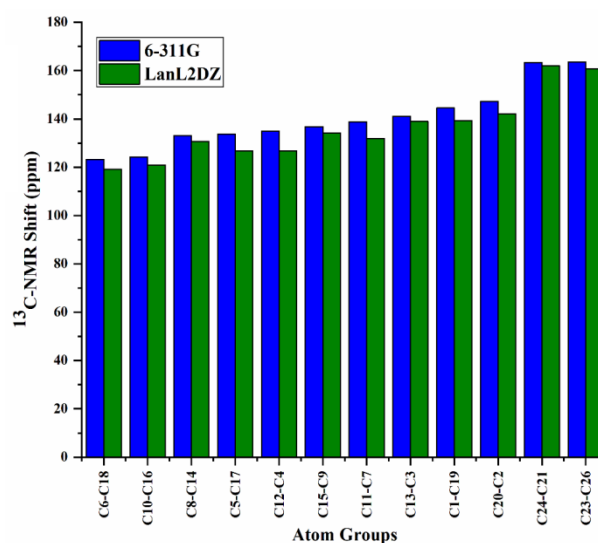


Figure 9. ¹³C NMR chemical shift graph of DBP compound.

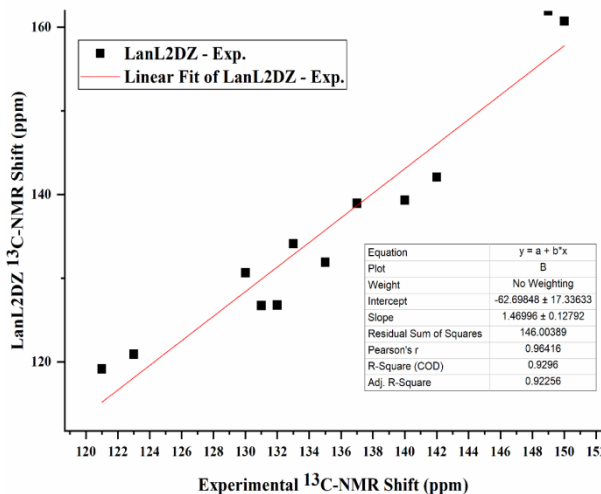
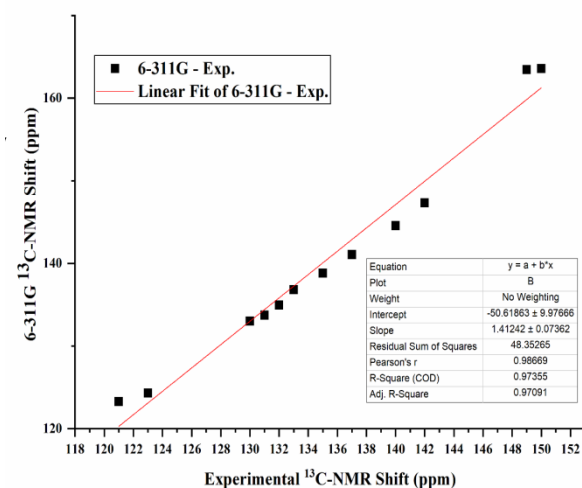


Figure 10. Correlation graph of ¹³C-NMR experimental and theoretical results of DBP compound.

Table 3. DFT-B3LPY / 6-311G (d, p) and LanL2DZ ¹³C- NMR theoretical results for DBP molecule.

Atoms	Experi- mental	6-311G	LanL2DZ
	Shift (ppm)	Shift (ppm)	Shift (ppm)
C6-C18	121	123.29	119.15
C10-C16	123	124.32	120.91
C8-C14	130	133.02	130.65
C5-C17	131	133.73	126.73
C12-C4	132	134.96	126.80
C15-C9	133	136.83	134.14
C11-C7	135	138.82	131.90
C13-C3	137	141.05	138.95
C1-C19	140	144.59	139.33
C20-C2	142	147.33	142.10
C24-C21	149	163.43	161.97
C23-C26	150	163.57	160.73

Table 4. For DBP molecule, DFT-B3LPY / 6-311G (d, p) and LanL2DZ ¹H-NMR theoretical results are given.

Atom Groups	Experimental	6-311G	LanL2DZ
	Shift-(ppm)	Shift-(ppm)	Shift-(ppm)
37-35	8.71-8.91	8.91	8.00
38-33	7.03	9.02	7.85
36-34	9.51	9.57	7.98

DFT method and HOMO -7.10 eV - LUMO -4.60 eV for the LanL2DZ method were calculated from the figure. For other orbitals; HOMO₋₁ -8.06 eV - LUMO₊₁ 3.02 eV for the DFT method and HOMO₋₁ -8.19 eV - LUMO₊₁ 3.19 eV for the LanL2DZ method were calculated. Because, properties such as molecular orbitals (HOMO-LUMO) and energy are very useful for physicists and chemists and are very important for quantum chemistry. Analyses of boundary molecular orbitals define an electron impulse from the HOMO to the LUMO. The energy of HOMO is directly related to its ionization potential, and the energy of LUMO is directly related to the electron affinity. The HOMO and LUMO energy gap explains the possible charge transfer in the interaction with molecules. A boundary orbital space with a molecule is often linked to high chemical reactivity, low kinetic stability, and softly expressed molecules. HOMO and LUMO orbitals determine how the molecule interacts with other compounds. It also helps to characterize band gap, chemical reactivity and kinetic stability. A small boundary shows the polarization, stiffness, electronegativity and other reactivity indices of a molecule with an orbital space. Table 5 shows the chemical reactivity indices.

Table 5. Comparison of HOMO-LUMO, band gaps (HOMO - LUMO) and related DBP (eV) chemical properties.

Molecular Energy	6-311G	LanL2DZ
LUMO	-4.42	-4.60
HOMO	-6.97	-7.09
(ΔE) Band Gaps	-2.55	-2.49
($I = -E_{\text{HOMO}}$)	6.97	7.09
($A = -E_{\text{LUMO}}$)	4.42	4.60
($\eta = (A - I) / 2$)	1.27	1.25
($s = I / 2 \eta$)	0.64	0.62
($\mu = -\chi$)	-5.69	-5.85
($\chi = (I + A) / 2$)	5.69	5.85
($\omega = \mu^2 / 2 \eta$)	12.75	13.69

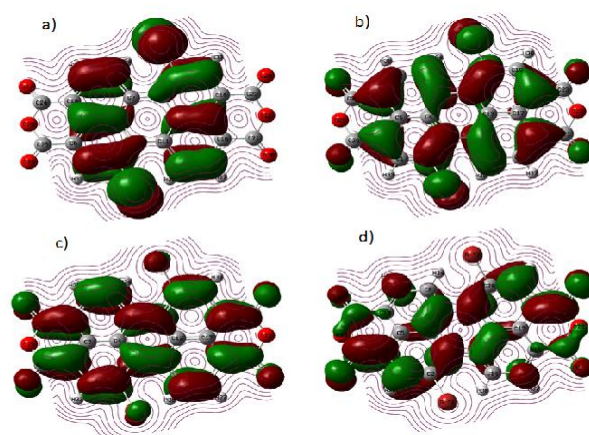
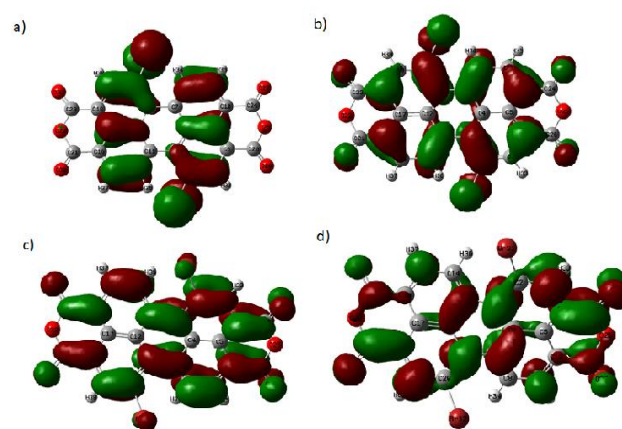
**Figure 11.** For the DBP molecule a) DFTHOMO₋₁, b) DFT_{HOMO}, c) DFT_{LUMO}, d) DFT_{LUMO+1}**Figure 12.** For the DBP molecule: a) LanL2DZ HOMO₋₁, LanL2DZ HOMO, c) LanL2DZ LUMO, d) LanL2DZ LUMO₊₁

Table 6. The basic set of LanL2DZ with DFT is B3LYP / 6-31G (d, p), dipole moments, polarizability, β components of dibromide perylene value.

Parameters	6-311G	LanL2DZ	Parameters	6-311G	LanL2DZ
μ_x	0.0001	-0.0001	β_{xxx}	-0.0111	-0.0699
μ_y	0.0005	0.0005	β_{xxy}	0.0126	0.0198
μ_z	-0.0796	-0.0619	β_{xyy}	0.0214	-0.0165
$\mu(D)$	0.0796	0.0619	β_{yyy}	0.0170	0.0313
α_{xx}	-297.1694	-307.3846	β_{xxz}	-65.4351	-84.3452
α_{yy}	-202.1148	-197.0362	β_{xyz}	-31.3278	-31.7962
α_{zz}	-202.4589	-196.8185	β_{yyz}	-32.0949	-36.3150
α_{xy}	-14.8213	-0.0016	β_{xzz}	-0.0200	0.0010
α_{xz}	-0.0003	0.0016	β_{yzz}	-0.0111	-0.0002
α_{yz}	-0.0054	-0.0016	β_{zzz}	-55.9040	-75.1277
$\alpha(\text{au})$	-233.9143	-233.7464	$\beta(\text{esu})$	153.43×10^{-29}	195.78×10^{-29}

Dipole moment is an important feature of the energy related to the electric field applied in the molecule.³⁰ Basically, the dipole moment consists of intermolecular interactions involving the Van der Waals type dipole-dipole forces and generates strong intermolecular attraction. Table 6 shows the calculated parameters, the electronic dipole moment and the total dipole moment. Dipole moment, molecular polarization and hyper polarizability values are important in determining the properties of nonlinear optics (NLR).

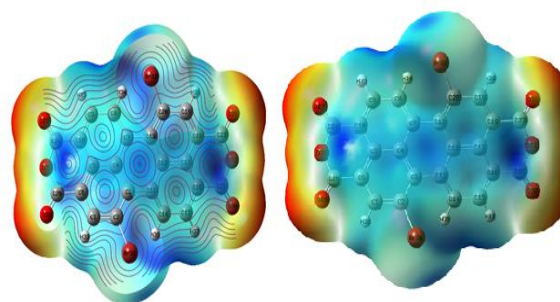
3.4. Molecular electrostatic potential surface (MESP)

The molecular electrostatic potential surface, MESP shows the shape, size and electrostatic potential values of the molecule and is plotted for the dibromide perylene molecule. MESP mapping is very useful in investigating the physicochemical properties of molecular structure.³¹ A portion of the molecule with negative electrostatic potential is sensitive to electrophilic attack.

The red and blue regions on the MESP map correspond to the negative and positive potential regions and refer to electron rich and electron deficient regions respectively. The green color indicates neutral electrostatic potential.

In this study, MESP were mapped for the DBP molecule as shown in Figure 13. In the case of dibromide perylene, the MESP map shows that there are negative potential zones characterized by red color around the oxygen atoms. A relatively larger region around the oxygen atoms of the dibromide perylene molecule represents the most negative potential region (dark red) and is permissible for electrophilic interaction. The hydrogen atom carries the maximum force of the positive charge (dark blue).

It shows an almost neutral potential as most of the aromatic ring region is represented by green.

**Figure 13.** Molecular electrostatic potential and contour maps for the DBP molecule.

3.5. Mulliken atomic charges

Determination of Mulliken atomic charge is an important parameter in quantum chemical calculations. Because, it affects many features such as atomic charges, dipole moment, molecular polarization and electronic structure in the molecule. It also shows the formation of electron donor and receiver pairs along with charge distribution and intra-molecular charge transfer. Mulliken atom was calculated in the B3LYP / 6-311G (d, p) basis set of DFT and LanL2DZ methods. The data are presented in Figures 14 and 15, and Table 7. The distribution of the Mulliken atomic charge is that the oxygen atom attached to the aromatic ring is O27 (-0.22) - (-0.19), O25 (-0.20) - (-0.25), O29 (-0.22) - (-0.19), O28 (-0.23) - (-0.19), and O30 (-0.22) - (-0.19) have a negative charge. The charge value of the H atom attached to the aromatic ring has a positive charge. Some C atoms were observed to be negative and others positive.

Table 7. Mulliken atomic charges were calculated with DFT and LanL2DZ B3LYP / 6-31G (d, p)

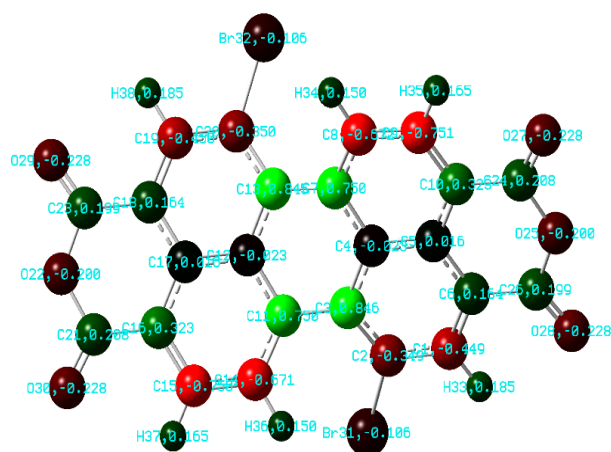
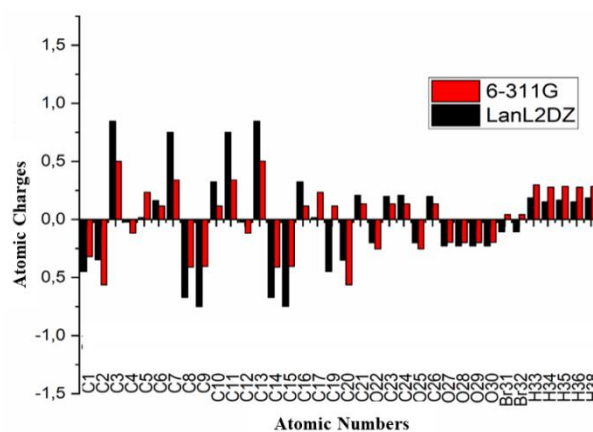
	6-311G	LanL2DZ		6-311G	LanL2DZ
C1	-0.45	-0.32	C20	-0.3	-0.56
C2	-0.35	-0.56	C21	0.20	0.13
C3	0.85	0.50	O22	-0.20	-0.25
C4	-0.02	-0.12	C23	0.19	0.13
C5	0.01	0.23	C24	0.21	0.13
C6	0.16	0.12	O25	-0.20	-0.25
C7	0.75	0.34	C26	0.19	0.13
C8	-0.67	-0.41	O27	-0.22	-0.19
C9	-0.75	-0.41	O28	-0.22	-0.19
C10	0.32	0.12	O29	-0.22	-0.19
C11	0.75	0.34	O30	-0.22	-0.19
C12	-0.02	-0.12	Br31	-0.10	0.04
C13	0.84	0.50	Br32	-0.10	0.04
C14	-0.67	-0.41	H33	0.18	0.29
C15	-0.75	-0.40	H34	0.15	0.27
C16	0.32	0.11	H35	0.16	0.28
C17	0.016	0.23	H36	0.15	0.27
C19	-0.45	0.11	H38	0.18	0.28

3.6. Natural orbital bond (NBO) analysis

The natural orbital bond (NBO) analysis provides research on the most accurate lewis structure of the molecule, detailed electron density of all orbitals. The NBO method is an evaluation of full and empty orbital interactions that provide information about both intra- and intermolecular interactions. In order to evaluate the donor-acceptor interactions in the NBO analysis of our compound, a second order Fock matrix was performed.

NBO calculation is used to understand the other second order interactions between the filled orbits of one subsystem and the empty orbitals of another subsystem. These results are delocalization and hyperconjugation measurements. The analyzed results are given in Table 8.

Intramolecular interactions are observed as an increase in electron density (ED) in antibody orbitals that weaken the relevant bonds (C-O). The electron density of the conjugated substituted bond (1.9734 au) clearly shows a strong delocalization. The occupancy rate of σ bonds is higher than σ^* bonds, which provides more localization.

**Figure 14.** Mulliken atomic charges for the DBP molecule.**Figure 15.** Comparison of Mulliken atomic charges for DBP molecule.

The intramolecular hyperconjugative interaction of the distribution to π (C2-C3) electrons in the ring leads to a stabilization of a portion of the ring as is evident from Table 8. Intramolecular hyperconjugative interaction of π^* (C1-C6) and anti π^* (C4-C5) in the ring leads to stabilization of 18.95 kcal mol⁻¹. These values increased conjugation leading to strong localization.

4. CONCLUSION

In this study, the spectroscopic characterization of 5, 12 Dibromo perylene (DBP) was performed. Detailed investigations were made theoretically using quantum chemical calculations for DBP molecule. The structural, electronic, vibration frequencies of the compound were calculated with the basic set of DFT-B3LYP / 6-311G (d, p) and LanL2DZ. The structural parameters (bond lengths, bond angles and dihedral angles) were determined.

Table 8. Selected NBO results show the formation of Lewis and non-Lewis orbitals for the DBP molecule using the DFT B3LYP / 6-311 G ++ (d, p) theory level

NBO(i)	Type	ED/e	NBO(j)	Type	ED//e	E(2) ^a (Kcal/mol)	E (j)-E(i) ^b (a.u.)	F (i, j) ^c (a.u)		
C1-C2	σ	1.97742	C6-C1	σ^*	0.02248	3.69	1.30	0.062		
			H33-C1	σ^*	0.01530	1.26	1.13	0.034		
			C3-C2	σ^*	0.03455	4.53	1.28	0.068		
			C11-C3	σ^*	0.03468	3.95	1.20	0.062		
			C26-C2	σ^*	0.07304	3.47	1.10	0.056		
C1-C6	σ	1.96536	C2-C1	σ^*	0.02445	3.66	1.24	0.060		
			H33- C1	σ^*	0.01530	1.43	1.14	0.036		
			Br31 - C2	σ^*	0.03589	4.48	0.81	0.054		
			C6 - C5	σ^*	0.03200	4.95	1.25	0.070		
			C5-C10	σ^*	0.03287	2.89	1.25	0.054		
			C6-C26	σ^*	0.07304	2.21	1.10	0.044		
			C26- O25	σ^*	0.12693	1.32	0.98	0.033		
			O28- C26	σ^*	0.01934	0.72	0.83	0,024		
			π	1.69323	C3- C2	π^*	0.38644	16.07	0.28	0.061
					C5- C4	π^*	0.43123	18.95	0.30	0.069
					C26- O25	π^*	0.12693	1.02	0.52	0.022
O28- C26	π^*	0.17789			16.51	0.25	0.060			
C1-H33	σ	1.97542	C2 -C1	σ^*	0.02445	0.66	1.02	0.023		
			C6-C1	σ^*	0.02248	1.03	1.09	0.030		
			C3-C2	σ^*	0.03455	4.88	1.07	0.065		
			C6-C5	σ^*	0.03200	5.15	1.04	0.065		
C2-Br31	σ	1.98238	C6-C1	σ^*	0.02248	2.80	1.27	0.053		
			C4-C3	σ^*	0.03314	4.15	1.21	0.063		
C19-H38	σ	1.97541	C20- C13	σ^*	0.03453	4.88	1.07	0.065		
			C18- C17	σ^*	0.03203	5.16	1.03	0.065		
			C19- C18	σ^*	0.02249	1.03	1.09	0.030		
			C19-C20	σ^*	0.02444	0.66	1.02	0.023		
C21-O22	σ	1.97328	C16- C15	σ^*	0.02261	1.50	1.42	0.041		
			O22- C21	σ^*	0.12895	0.56	1.09	0.023		
			O29-C23	σ^*	0.01947	1.45	1.40	0.040		
			O29-C23	σ^*	0.17658	2.91	0.82	0.045		
C21-O30	σ	1.99496	C17- C16	σ^*	0.037	1.01	1.64	0.037		
			C21-C16	σ^*	0.049	1.93	1.48	0.049		
			C23-O22	σ^*	0.030	0.76	1.36	0.030		
			π	1.98104	C16-C15	π^*	0.28027	3.75	0.42	0.038
O22-C23	π^*	0.12708			0.90	0.64	0.022			
C24-O25	σ	1.97345	C10- C9	σ^*	0.02261	1.50	1.42	0.041		
			O25-C24	σ^*	0.12890	0.56	1.09	0.023		
			O28- C26	σ^*	0.01934	1.47	1.40	0.040		
			O28- C26	σ^*	0.17789	2.88	0.82	0.045		
C24-O27	σ	1.99494	C10-C5	σ^*	0.03287	1.01	1.63	0.037		
			C24-C10	σ^*	0.07329	1.94	1.48	0.049		
			C26- O25	σ^*	0.12693	0.76	1.36	0.030		
			π	1.98101	C10- C9	π^*	0.28011	3.76	0.42	0.038
C26- O25	π^*	0.12693			0.90	0.64	0.022			
O25-C26	σ	1.97337	C6-C1	σ^*	0.02248	1.55	1.42	0.042		
			O27-C24	σ^*	0.01949	1.45	1.40	0.040		
			O27-C24	σ^*	0.17666	2.90	0.82	0.045		
			C26-O25	σ^*	0.12693	0.54	1.09	0.022		

Nonlinear optical properties were investigated. Finally, it was concluded that the compound examined could be used as a nonlinear optical (NLO) material. Because polarity ($\alpha = -233.9143$ au and $\alpha = -233.7464$ au) and static high-order polarity ($\beta = 153.43 \times 10^{-29}$ esu and $\beta = 195.78 \times 10^{-29}$ esu) parameters were determined from the calculations for the DBP molecule. The theoretically high degree of polarity values from the data obtained for

the DBP molecule were considered to be a good candidate for nonlinear optical materials. In addition, MESP, HOMO-LUMO maps and Mulliken loads were visualized. It is available as a good intermediate material for syntheses. That is, the fact that the material is formed in the reaction and can be used in the next step means that the material is a good intermediate product in the reactions with mechanisms. Thus, by

DOI: <http://dx.doi.org/10.32571/ijct.695754>

E-ISSN:2602-277X

taking these data into consideration for future synthesis studies, this study will provide important facilities for the synthesis of molecules by minimizing the chemical consumption of the molecules to be synthesized in the future and making necessary predictions.

Conflict of interests

Authors declare that there is no a conflict of interest with any person, institute, company, etc.

REFERENCES

- Paredes-Gil, K.; Mendizabal, F.; Páez-Hernández, D.; Arratia-Pérez, R. *Comput. Mater. Sci.* **2017**, 126, 514-527.
- Kolcu, F.; Çulhaoğlu, S.; Kaya, İ. *Prog. Org. Coat.* **2019**, 137, 105284.
- Kucinska, M.; Frac, I.; Ulanski, J.; Makowski, T.; Nosal, A.; Gazicki-Lipman, M. *Synth. Met.* **2019**, 250, 12-19.
- Dong, D.; Li, Q.; Hou, W.; Zhang, H. *J. Mol. Struct.* **2020**, 1199, 127002.
- Cao, L.; Xu, L.; Zhang, D.; Zhou, Y.; Zheng, Y.; Fu, Q.; Jiang, X.-F.; Lu, F. *Chem. Phys. Lett.* **2017**, 682, 133-139.
- Otero, R.; Vázquez De Parga, A. L.; Gallego, J. M. *Surf. Sci. Rep.* **2017**, 72 (3), 105-145.
- Dere, A. *Physica B Condens. Matter.* **2018**, 547, 127-133.
- Veerababu, M.; Kothandaraman, R. *Electrochim. Acta.* **2017**, 232, 244-253.
- Djurišić, A. B.; Fritz, T.; Leo, K. *Opt. Commun.* **2000**, 183 (1), 123-132.
- Farag, A. A. M.; Osiris, W. G.; Yahia, I. S. *Synth. Met.* **2011**, 161 (17), 1805-1812.
- Büyükekşi, S. I.; Orman, E. B.; Acar, N.; Altındal, A.; Özkaya, A. R.; Şengül, A. *Dyes Pigments* **2019**, 161, 66-78.
- Ozser, M. E.; Mohiuddin, O. *J. Mol. Struct.* **2018**, 1158, 145-155.
- Lathiotakis, N. N.; Kerkines, I. S. K.; Theodorakopoulos, G.; Petsalakis, I. D. *Chem. Phys. Lett.* **2018**, 691, 388-393.
- Cabir, B.; Yildiko, U.; Ağırtaş, M. S. *J. Coord. Chem.* **2019**, 72 (17), 2997-3011.
- Basma, A.-K.; Dinleyici, M.; Abourajab, A.; Kök, C.; Bodapati, J. B.; Uzun, D.; Koyuncu, S.; Icil, H. *J. Photoch Photobio A.* **2020**, 393, 112432..
- Solğun, D. G.; Keskin, M. S.; Yıldiko, Ü.; Ağırtaş, M. S. *Chem. Pap.* **2020**, 74, 2389-2401.
- M. J. Frisch, G. W. T., H. B. Schlegel, G. E. Scuseria, M. A. Robb, J. R. Cheeseman, G. Scalmani, V. Barone, G. A. Petersson, H. Nakatsuji, X. Li, M. Caricato, A. Marenich, J. Bloino, B. G. Janesko, R. Gomperts, B. Mennucci, H. P. Hratchian, J. V. Ortiz, A. F. Izmaylov, J. L. Sonnenberg, D. Williams-Young, F. Ding, F. Lipparini, F. Egidi, J. Goings, B. Peng, A. Petrone, T. Henderson, D. Ranasinghe, V. G. Zakrzewski, J. Gao, N. Rega, G. Zheng, W. Liang, M. Hada, M. Ehara, K. Toyota, R. Fukuda, J. Hasegawa, M. Ishida, T. Nakajima, Y. Honda, O. Kitao, H. Nakai, T. Vreven, K. Throssell, J. A. Montgomery, Jr., J. E. Peralta, F. Ogliaro, M. Bearpark, J. J. Heyd, E. Brothers, K. N. Kudin, V. N. Staroverov, T. Keith, R. Kobayashi, J. Normand, K. Raghavachari, A. Rendell, J. C. Burant, S. S. Iyengar, J. Tomasi, M. Cossi, J. M. Millam, M. Klene, C. Adamo, R. Cammi, J. W. Ochterski, R. L. Martin, K. Morokuma, O. Farkas, J. B. Foresman, And D. J. Fox, *Gaussian 09, Revision A.02, Gaussian, Inc., Wallingford Ct*, 2016.
- Khajehzadeh, M.; Moghadam, M. *Spectrochim. Acta A:* **2017**, 180, 51-66.
- Miehlich, B.; Savin, A.; Stoll, H.; Preuss, H. *Chem. Phys. Lett.* **1989**, 157 (3), 200-206.
- Hertwig, R. H.; Koch, W. *Chem. Phys. Lett.* **1997**, 268 (5-6), 345-351.
- Hay, P. J.; Wadt, W. R. *J. Chem. Phys.* **1985**, 82 (1), 270-283.
- Ülküseven, B.; Bal-Demirci, T.; Akkurt, M.; Yalçın, Ş. P.; Büyükgüngör, O. *Polyhedron* **2008**, 27 (18), 3646-3652.
- Akkurt, M.; Yalçın, Ş.; Gürsoy, E.; Ulusoy Güzeldemirci, N.; Büyükgüngör, O. *Acta Crystallogr. E.* **2007**, 63, O3103.
- Matussek, M.; Filapek, M.; Gancarz, P.; Krompiec, S.; Grzegorz Małeck, J.; Kotowicz, S.; Siwy, M.; Maćkowski, S.; Chrobok, A.; Schab-Balcerzak, E.; Słodek, A. *Dyes Pigments* **2018**, 159, 590-599.
- Li, H.; Meng, J.; Sun, X. *Inorg. Chem. Commun.* **2019**, 105, 194-198.

DOI: <http://dx.doi.org/10.32571/ijct.695754>

E-ISSN:2602-277X

26. Huang, C.; Barlow, S.; Marder, S. R. *J. Org. Chem.* **2011**, 76 (8), 2386-2407.

27. Paksresht, M.; Bodapati, J. B.; Icil, H. *J. Photochem. Photobiol. A.* **2018**, 360, 270-277.

28. Wu, S.; Cheng, C.; Hou, W.; Li, Q.; Dong, D.; Gao, Y.; Liu, L.; Liang, B.; Zhang, H. *Tetrahedron* **2019**, 75 (41), 130577.

29. Yuen, J. D.; Pozdin, V. A.; Young, A. T.; Turner, B. L.; Giles, I. D.; Naciri, J.; Trammell, S. A.; Charles, P. T.; Stenger, D. A.; Daniele, M. A. *Dyes Pigments* **2019**, 108014.


30. Piosik, E.; Synak, A.; Martyński, T. *Spectrochim. Acta A: Mol. Biomol. Spectrosc.* **2018**, 189, 374-380.


31. Pekdemir, F.; Orman, E. B.; Selçuki, N. A.; Özkaya, A. R.; Salih, B.; Şengül, A. *J. Photochem. Photobiol. A* **2019**, 379, 54-6.

ORCID

 <https://orcid.org/0000-0003-3345-6445> (M. Akman)

 <https://orcid.org/0000-0002-2296-2265> (A. Ç. Ata)

 <https://orcid.org/0000-0001-8627-9038> (Ü. Yıldiko)

 <https://orcid.org/0000-0002-3191-7570> (İ. Çakmak)